X-651-71-463
PREPRINT

NASA TM X- 65774

GLOBAL DISTRIBUTION OF TOTAL OZONE DERIVED FROM NIMBUS 3 SATELLITE DURING APRIL-JULY, 1969 AND ITS IMPLICATION TO UPPER TROPOSPHERIC CIRCULATION

C. PRABHAKARA
E. B. RODGERS
V. V. SALOMONSON

NOVEMBER 1971

GODDARD SPACE FLIGHT CENTER
GREENBELT, MARYLAND

X-651-71-463

GLOBAL DISTRIBUTION OF TOTAL OZONE DERIVED FROM NIMBUS 3 SATELLITE DURING APRIL-JULY, 1969 AND ITS IMPLICATION TO UPPER TROPOSPHERIC CIRCULATION

C. Prabhakara

E. B. Rodgers*

V. V. Salomonson

November 1971

*Allied Research Associates.

GODDARD SPACE FLIGHT CENTER
Greenbelt, Maryland

GLOBAL DISTRIBUTION OF TOTAL OZONE DERIVED FROM NIMBUS 3 SATELLITE DURING APRIL-JULY, 1969 AND ITS IMPLICATION TO UPPER TROPOSPHERIC CIRCULATION

C. Prabhakara

E. B. Rodgers

V. V. Salomonson

ABSTRACT

Utilizing a stepwise multiple regression scheme monthly mean global maps of total ozone are produced from the spectral intensity measurements made by Infrared Interferometer Spectrometer (IRIS) onboard the Nimbus 3 satellite for the period April 18 to July 22, 1969. These maps show that over the equatorial regions total ozone increases steadily from April to July. Further, latitudinal variation of total ozone derived from these maps shows that the ozone increases at all latitudes over the southern hemisphere uniformly from April to July while over the northern hemisphere the monthly decrease at all latitudes is nonuniform. In general, these maps bear a close resemblance to the upper tropospheric circulation. It is observed that the total ozone is best correlated with the 200 mb geopotential heights. This relationship enables us to utilize total ozone as a quasi-stream function to determine geostrophic winds at 200 mb level. Further, even at low latitudes where the total ozone does not bear simple relationship to the geopotential heights we can identify the course of the easterly jet stream with the help of the ozone measurements.

CONTENTS

ILLUSTRATIONS

GLOBAL DISTRIBUTION OF TOTAL OZONE DERIVED FROM NIMBUS 3 SATELLITE DURING APRIL-JULY, 1969 AND ITS IMPLICATION TO UPPER TROPOSPHERIC CIRCULATION

1. INTRODUCTION

Ozone in the earth's atmosphere is produced photochemically by the solar near ultraviolet radiation. However, the global distribution of total ozone as a function of latitude and season cannot be explained by the corresponding changes in the solar radiation. On the contrary the atmospheric circulation plays a dominant role in the distribution of total ozone as a function of latitude and season. Since most of the ozone contained in the lower stratosphere (15-25 km) is not in photochemical equilibrium, total ozone changes are primarily produced by circulation in this layer (Craig, 1965, and Dutsch, 1969). Further, since the lower stratosphere is dynamically coupled to the upper troposphere (Peng, 1965), ozone becomes a useful tracer of the upper tropospheric circulation.

Several earlier studies (eq. London, 1963) based on conventional measurements of total ozone have attempted to demonstrate the importance of ozone as a tracer of global atmospheric circulation. However, the total ozone data available from conventional ground based measurements are quite sparse and limited to continental areas. With the advent of the polar orbiting meteorological satellite, Nimbus 3, it has been possible to sound the atmosphere and deduce the total ozone globally on a daily basis from the spectral measurements made by the high resolution Infrared Interferometer Spectrometer, IRIS, onboard this satellite. This method of determining the total ozone is based on a statistical regression

technique that greatly conserves the computing time necessary to process large amounts of data. A comprehensive discussion of determining total ozone from IRIS spectra is presented in the Appendix.

From IRIS measurements we have derived global total ozone maps for four consecutive months (April to July, 1969). These total ozone measurements are then used to obtain linear regression relations between total ozone and 200 mb geopotential heights over the mid-latitude regions of the northern and southern hemispheres. With these regression relations we have computed geostrophic winds. Isotach and streamline analysis are then constructed from the ozone derived geostrophic winds. From the streamline and isotach analysis large scale upper tropospheric circulation features such as the mid-latitude westerly jets over the northern and southern hemispheres are observed.

In the lower latitudes, however, simple relationship between total ozone and the 200 mb geopotential heights cannot be obtained. For this reason a quantitative analysis of the tropical easterly jet stream over the southeast Asia and north Africa could not be performed. Nevertheless, the easterly jet stream at the lower latitudes could be observed in a qualitative fashion from a fine spatial analysis of total ozone data along the jet axis.

2. TOTAL OZONE PATTERNS

The Nimbus 3 satellite orbited with a period of about 107 minutes from 80°N to 80°S and the successive orbits are displaced about 26° in longitude at the equator. The satellite is sun-synchronous, i.e., the satellite passes over most of the globe approximately at local noon or midnight. The retrogression of the satellite is

such that in about 7 days the orbits repeat their passes over roughly the same geographic location.

The IRIS instrument measured the infrared spectrum, over an approximately circular field of view of about 150 km in diameter, viewing vertically down along the subsatellite path. Each successive spectrum was taken about 16 sec. apart which corresponds to one spectrum for every 0.9° latitude spacing in the tropics. Obviously some overlap of geographic view from successive spectra is thus obtained. After taking 14 frames of consecutive spectra two spectra are missed, during which time calibration frames are taken (Nimbus Project, 1969).

The IRIS data obtained in this manner along the subsatellite path does not yield a simple synoptic picture consistent with a conventional meteorological scale of about 400 km. There is thus a need for us to choose a framework of space and time scales that are optimally suited to examine the IRIS data and the meteorological problem under consideration.

From the description of the satellite orbital geometry given above, it is readily seen that at low latitudes, when we combine IRIS data for one week there should be one measurement in each box of 1° latitude by 5° longitude. For several practical reasons data from a significant number of orbits are missing and so we have chosen to combine data for a period of two to three weeks. This procedure guarantees us a nearly complete coverage of data in a grid system of $1° \times 5°$.

A. Latitudinal Distribution

In order to appreciate the gross behavior of total ozone derived from the satellite over the globe we have constructed a latitudinal average for the four individual months (April-July, 1969) as shown in Figure 1. The four monthly total ozone curves are displaced 50 Dobson units apart along the ordinate in order to facilitate clarity for presentation.

From this figure we notice an equatorial minimum in total ozone for all the four months with an average of about 250 Dobson units increasing towards both poles. The position of this equatorial minimum is found to shift south of the equator to about 10°S during the time period April to July, 1969. The manner in which the total ozone changes from month to month is depicted by the dashed lines connecting the four monthly curves. Over the northern hemisphere it is seen that the total ozone is decreasing with latitude from April to July, while over the southern hemisphere the reverse is true. Further, the four monthly mean curves in the northern hemisphere tend to converge as one approaches higher latitudes, while in the southern hemisphere these monthly mean curves are parallel. The orientation of these curves suggests that in the southern hemisphere there is a uniform increase of total ozone from April to July, 1969, at all latitudes, while in the northern hemisphere on the other hand the monthly decrease of total ozone for the same period appears to be nonuniform. Presumably this difference between the orientation of the mean monthly curves of each hemisphere may be attributed to the difference of land and ocean configuration of the two hemispheres.

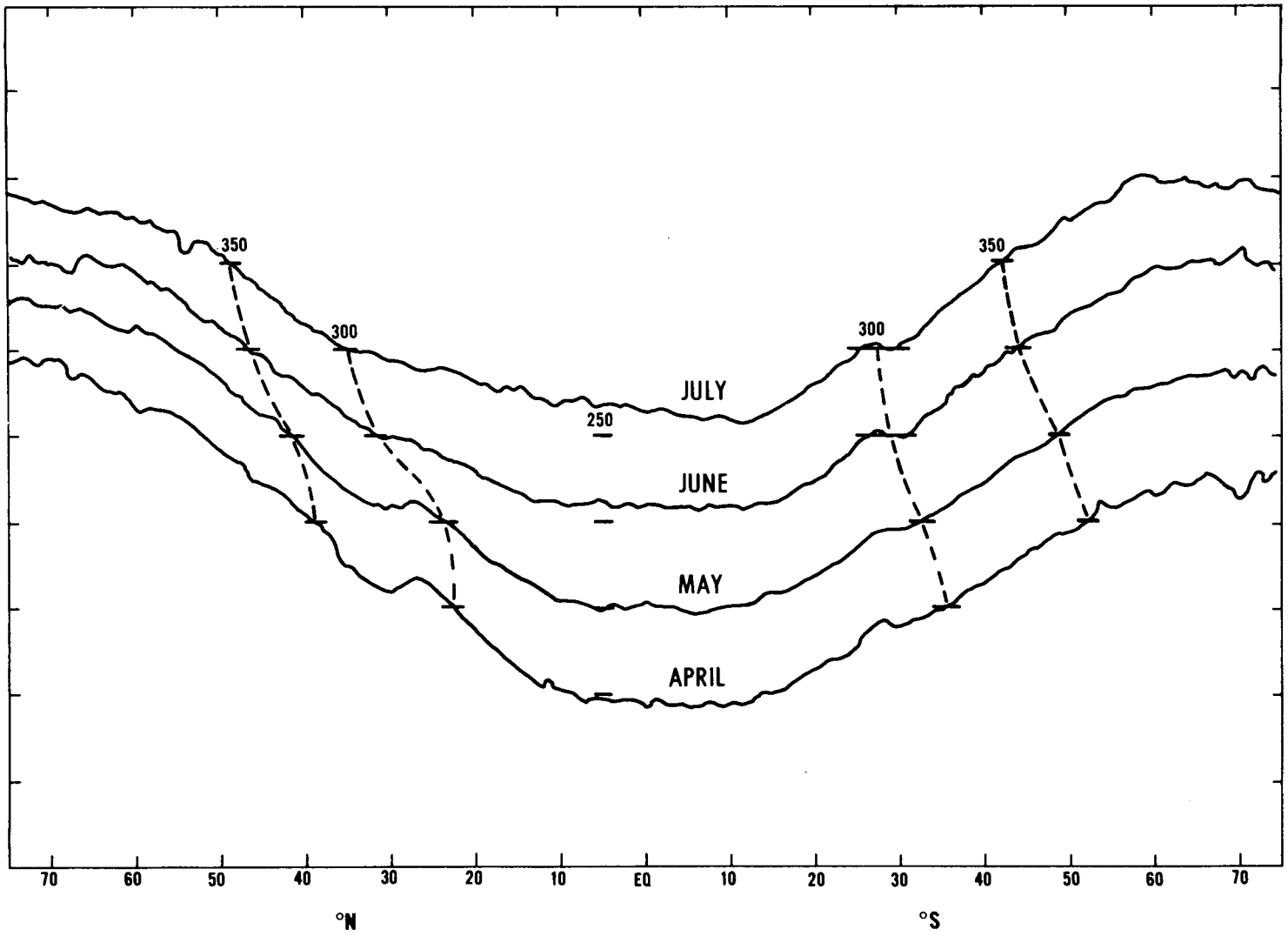

Figure 1. Latitudinal distribution of total ozone (10^{-3} cm STP) from Nimbus – 3 IRIS. The individual curves are displaced 50 Dobson units along the ordinate for facilitating presentation.

Also, from this figure one can notice significant secondary maxima of total ozone in the months of April and May at 30°N and another increase of total ozone at 30°S during all four months. These secondary maxima are a consequence of the mean position of the subtropical jet stream for each month over the northern and southern hemispheres. The absence of this feature at 30°N during June and July when the northern subtropical jet is weak further emphasizes the physical significance of these observations.

B. Monthly Mean Map Features

The four monthly mean global maps of total ozone for the period April to July 1969 are shown in Figures 2 through 5. The isopleths of total ozone are nearly parallel to latitude circles with ozone amounts increasing away from the equator towards both poles. The equatorial minimum in total ozone is produced by rising motion associated with the Hadley circulation in the lower stratosphere over the equatorial region (Murgatroyd and Singleton, 1961). In April the area in the tropics enclosed by the 250 Dobson Unit (D.U.) line runs nearly around the globe with a break between 60°E to 0° longitude. The size of this area decreases from April to July as the total ozone steadily increases through out the equatorial region and reaches values greater than 275 D.U. in the region 40°E to 20°W. These ozone variations surrounding the equator suggest that the Hadley circulation in the lower stratosphere is not symmetric.

The minimum in ozone observed over Tibetan Plateau and northeast India during the April and May is produced by the orographic influence of the Tibetan Plateau. Later on in summer months of June and July the sensible heat generated by the Tibetan Plateau and the latent heat released by the orographic uplift produce an

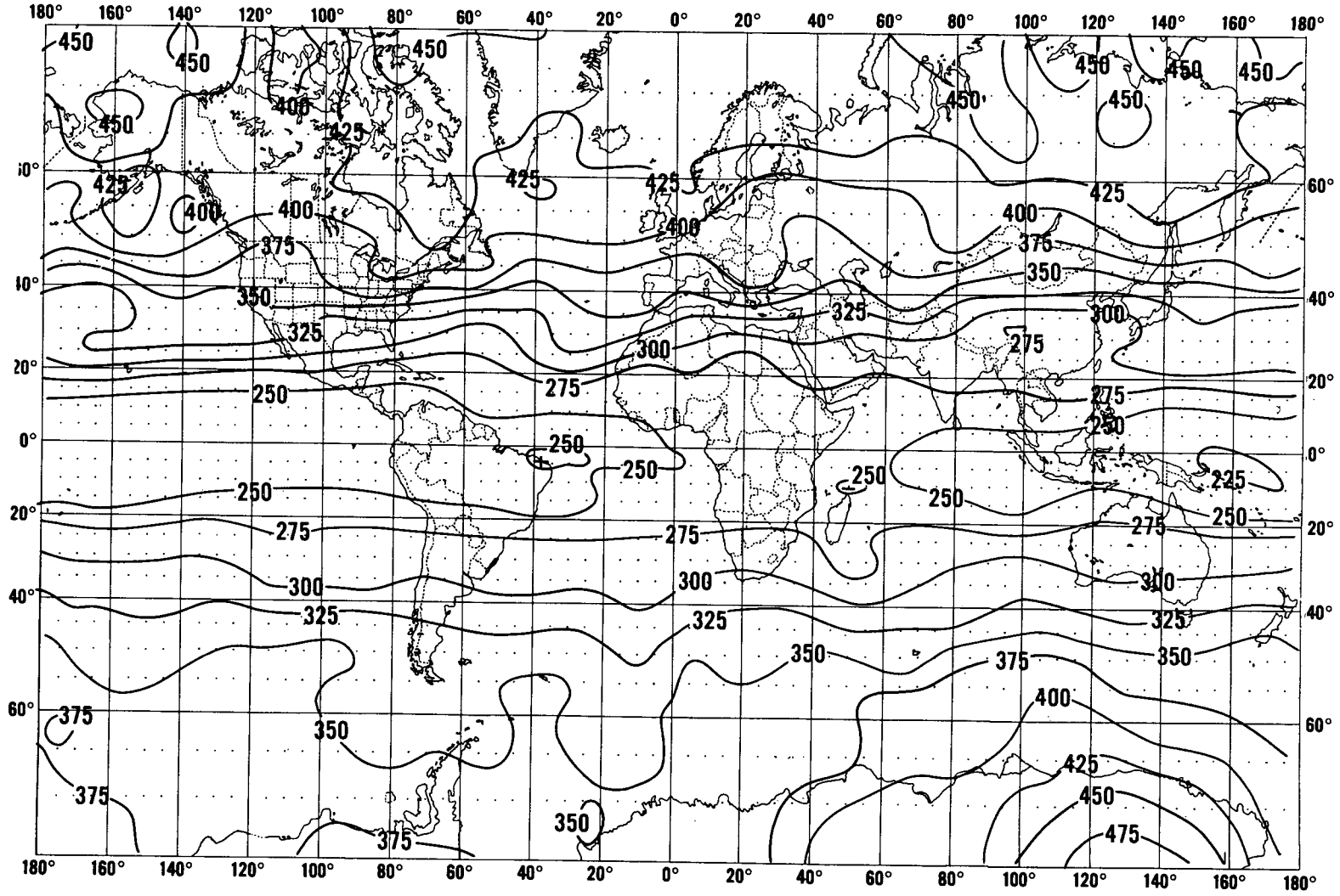

Figure 2. Global Distribution of Total Ozone for April 1969

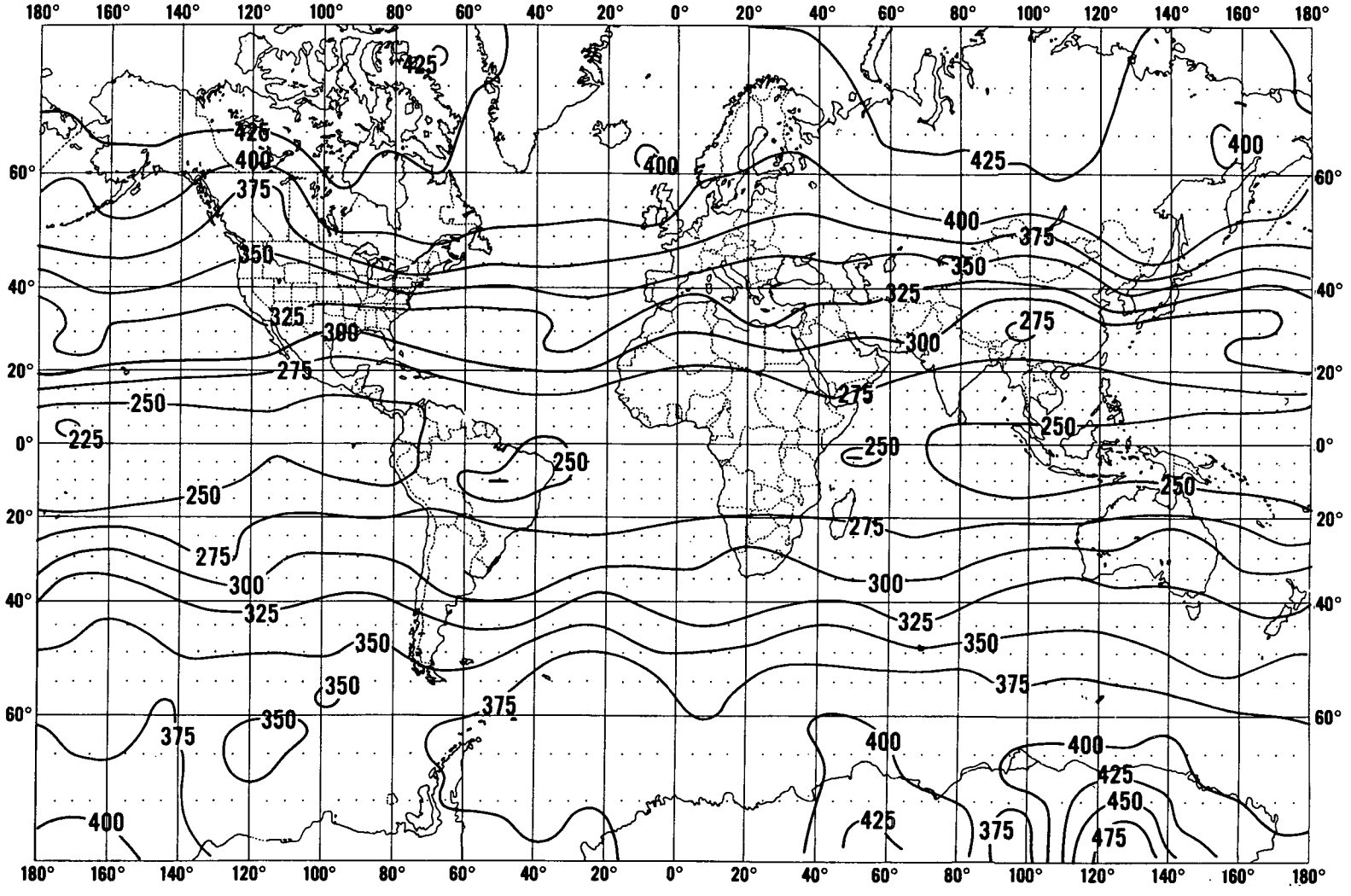

Figure 3. Global Distribution of Total Ozone for May 1969

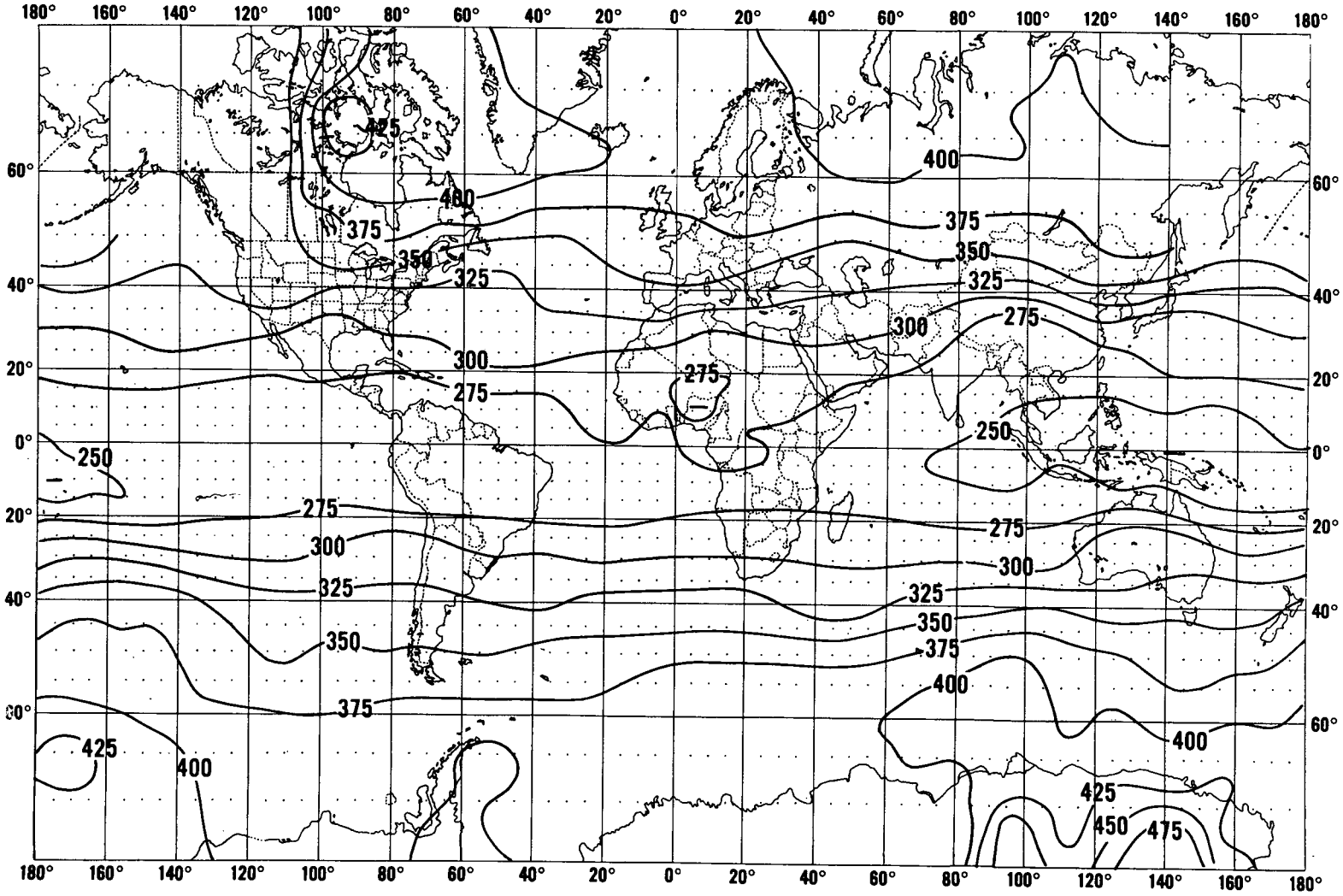

Figure 4. Global Distribution of Total Ozone for June 1969

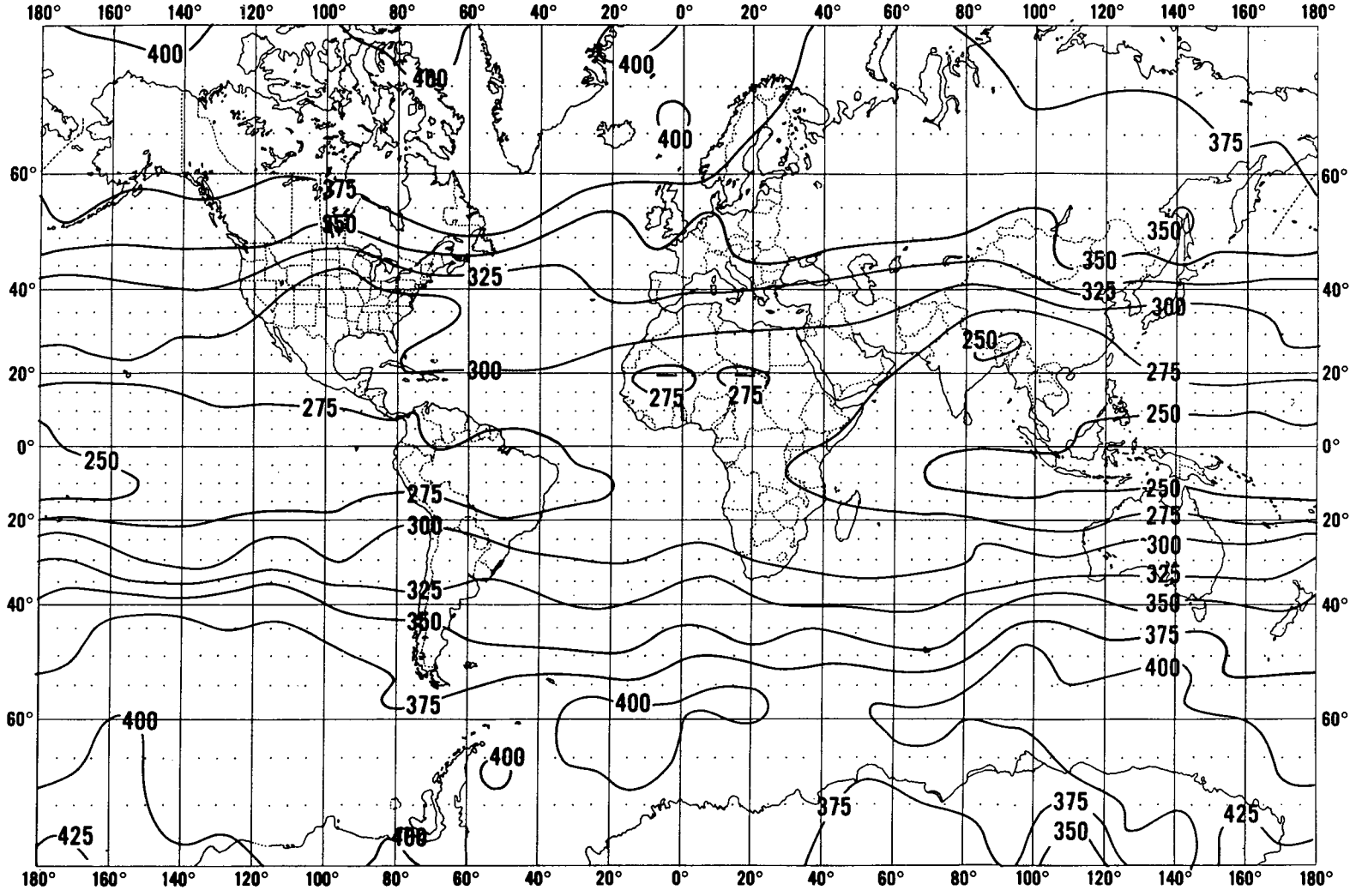

Figure 5. Global Distribution of Total Ozone for July 1969

anticyclone aloft (Murakami, 1963). In this anticyclone the horizontal divergence of ozone is not compensated adequately by subsidence motion and as a result an intense ozone minimum develops (Prabhakara et al., 1971). The existence of a total ozone minimum, in association with the upper air anticyclone, during July over the Mexican Plateau lends support to the above arguments. The ozone minima over Sahara region during June and July could be explained on similar grounds.

Over the mid latitude regions of the globe wave like patterns are revealed in the total ozone maps. These patterns reflect the large scale climatological features in the upper tropospheric flow. In particular one can notice in these maps two quasi-stationary "troughs"* over the northern hemisphere, one over the Atlantic and another over the Pacific. These "troughs" show a northeast to southwest tilt and further this tilt appears to increase from April to July. The position and behaviour of these quasi-stationary ozone "troughs" resemble closely the troughs in the 200 mb flow patterns shown by Krishnamurti (1970).

The distribution of total ozone in the southern hemisphere during April to July, 1969 shows significant zonal symmetry and no standing waves. These features suggest that the circulation in the lower stratosphere of the southern hemisphere is strongly zonal in character.

3. UPPER TROPOSPHERIC WINDS DERIVED FROM TOTAL OZONE DATA

A comparison of the monthly mean total ozone maps derived from the IRIS measurements with the corresponding upper air maps shows that the total ozone

* The shape of these "troughs" closely resembles conventional upper air troughs shown by geopotential height contours on constant pressure maps.

patterns resemble the distribution of upper air geopotential heights. In particular we find a high degree of correlation between 200 mb geopotential heights and the total ozone. We can take advantage of this relationship to specify the geopotential heights over the global regions where the radiosonde network is sparse and thereby derive the geostrophic winds.

The total ozone, O_3, can be related to the 200 mb geopotential heights, ϕ_{200}, by means of a linear regression equation as follows:

$$O_3 = C_0 + C_1 \phi_{200} \tag{1}$$

The two coefficients C_0 and C_1 are derived from our ozone data and the 200 mb geopotential heights taken from conventional upper air maps.

We can now form the geostrophic wind equations for u the east-west and v the north-south wind components.

$$u = -\frac{1}{f}\frac{\partial \phi_{200}}{\partial y} = -\frac{C_1}{f}\frac{\partial O_3}{\partial y}$$

$$v = \frac{1}{f}\frac{\partial \phi_{200}}{\partial x} = \frac{C_1}{f}\frac{\partial O_3}{\partial x} \tag{2}$$

where f is coriolis parameter.

Then total wind $\vec{V}$ and its direction θ are given by

$$\vec{V} = u^2 + v^2$$

$$\theta = \tan^{-1}\frac{v}{u} \tag{3}$$

We have deduced the 200 mb winds and directions over the globe utilizing Equations (2) and (3) from our ozone data. In Figure 6 the stream-line and isotach analysis of the wind data derived in this fashion for the month of July 1969 over the northern hemisphere is presented. Also in the same figure the 200 mb stream-line and isotach analysis of the July 1969 conventional wind data over the northern hemisphere is shown for comparison. The two analyses agree well. The mid-Atlantic and mid-Pacific troughs; the anticyclonic flow over Tibetan plateau, Mexican plateau and North Africa are evident in both the maps. This comparison proves our hypothesis that the total ozone can be used as a stream-function.

With this verification we can proceed to analyze the 200 mb flow over the southern hemisphere with the help of the IRIS measured total ozone data. In Figure 7 such an analysis of the isotachs and streamlines is presented. The strong westerly winds associated with the subtropical jet around 30°S and polar jet around 50°S are evident.

In order to observe the tropical easterly jet we have examined IRIS spectral data over a fine geographical grid of 1° latitude by 5° longitude. This type of scale would permit us to composit the data over long periods of time such as two or three weeks. If there are any persistent phenomena such as a jet stream over long enough periods of time it should be substantiated in such a composit map. The jet is not likely to be over a broad region and the fine scale would particularly favor delination of the jet like features.

In Figure 8 we have presented a map of the southeast Asia and Africa region with total ozone data composited in the manner described above for the period

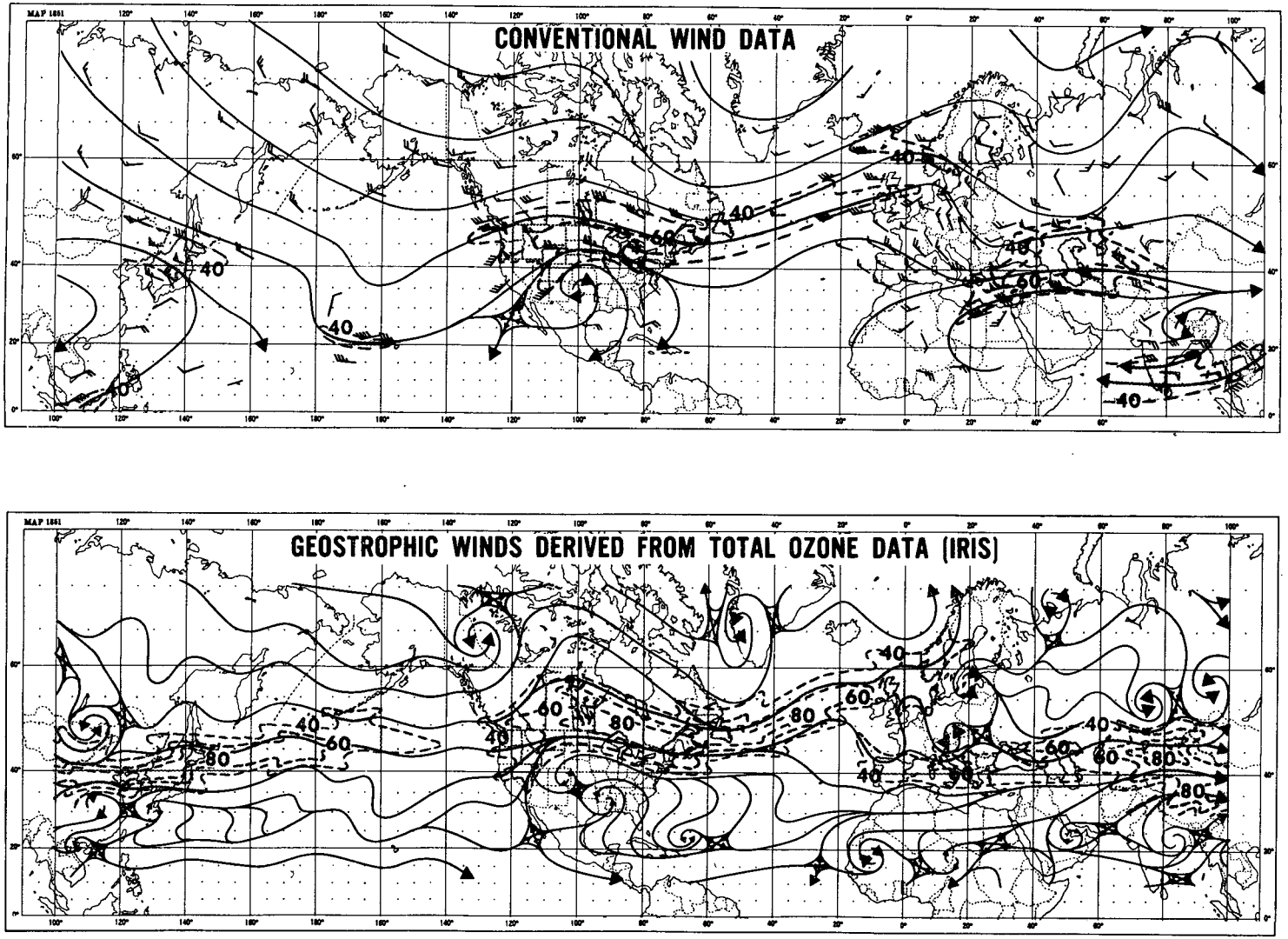

Figure 6. Comparison Between Geostrophic Winds Derived From Total Ozone IRIS Data and the Conventional Wind Data for the 200 mb Level Over the Northern Hemisphere During July 1969

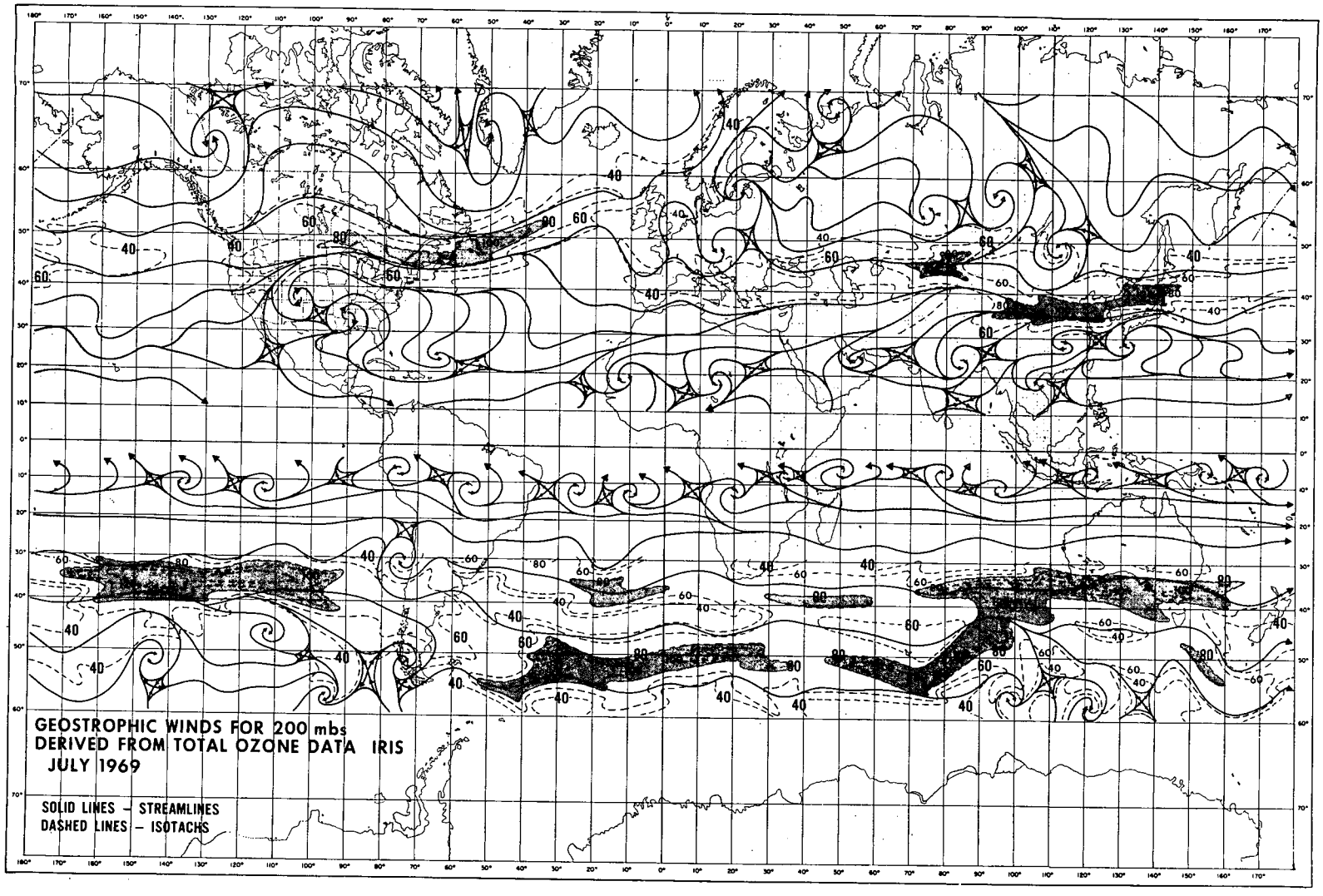

Figure 7. Geostrophic winds for the 200 mb level derived from total ozone IRIS data over the globe for the month of July 1969. Solid lines are streamlines and dashed are isotach.

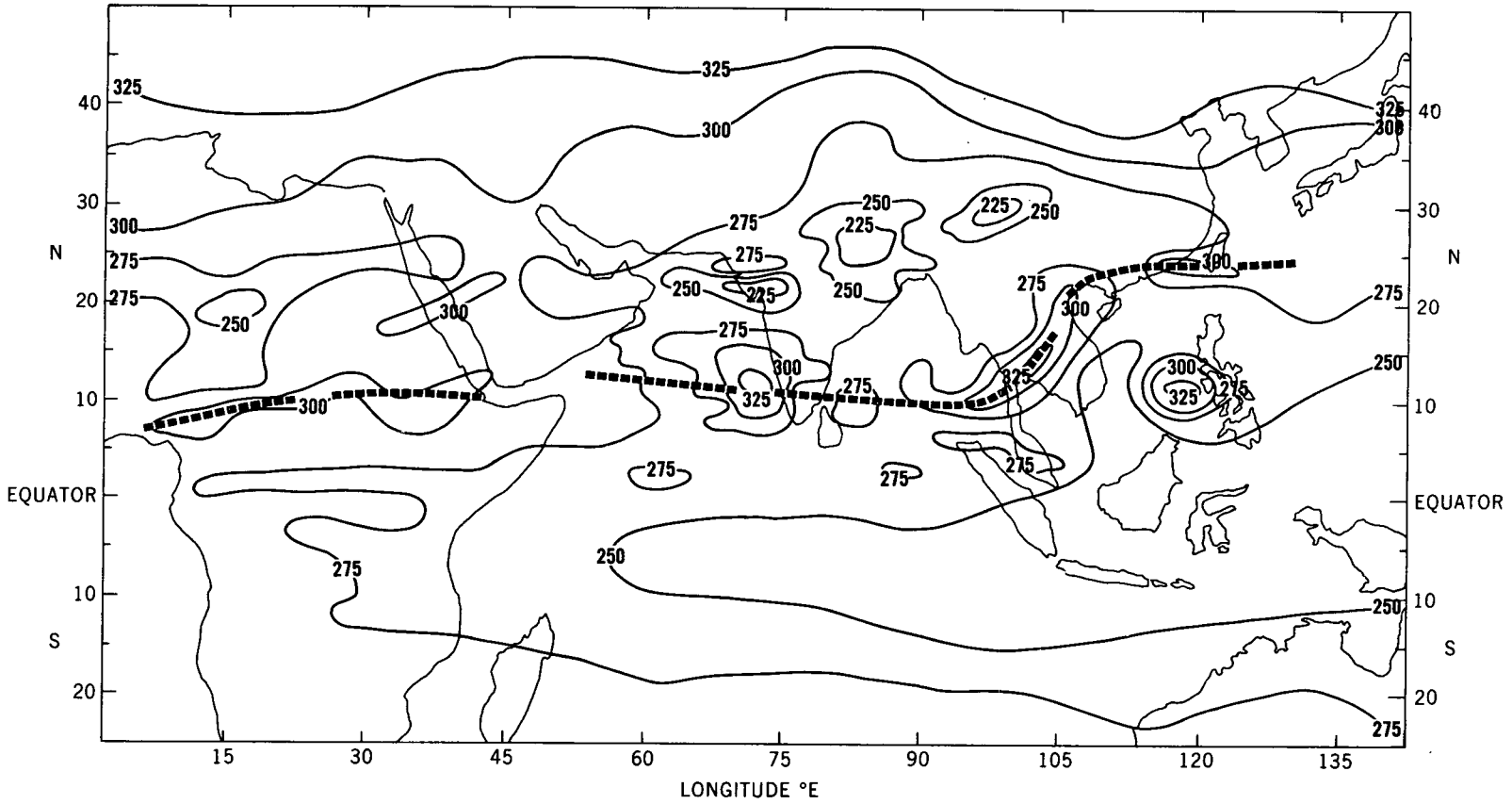

Figure 8. Total ozone distribution over Asia and Africa during 5–22 July 1969. Heavy dashed lines indicate the axes along which the ozone is a maximum. This axes corresponds to the track of the easterly jet.

July 5-22. Along the track of the easterly jet designated by heavy dashed lines, one can notice a maximum of total ozone apparently produced by the dynamics of the easterly jet. Over the southeast Asia and African region the total ozone maximum corresponds quite satisfactorily to the easterly jet studied by Kateswaram (1958).

4. CONCLUSION

The global distribution of ozone derived, from Nimbus 3 IRIS measurements, for the four months April, May, June, and July of 1969 reveal a systematic change in the lower stratospheric circulation. In particular, the Hadley circulation in the lower stratosphere appears to have a good zonal symmetry in April, however, by July such symmetry is lost.

The total ozone in the atmosphere is strongly correlated with the upper tropospheric geopotential heights. Utilizing this fact we have deduced the geostrophic winds at 200 mb level over the northern and southern hemisphere. The stream lines drawn from such data bear good resemblance to the upper air flow above 10° of latitude. The isotachs, however, are quantitatively reliable only above 30° of latitude. These winds reveal the subtropical and polar jet streams over the northern and southern hemispheres. The tropical easterly jet stream is observed from the ozone data in a qualitative fashion. We find along the track of the easterly jet stream the total ozone is a maximum.

The ozone distribution shows the quasi-stationary upper tropospheric long waves over the northern hemisphere. However, over the southern hemisphere such long waves do not appear. This difference between the two hemispheric circulations is attributable to the land ocean configuration.

From this study we have demonstrated that the total ozone measurements can provide useful meteorological information regarding the upper tropospheric flow over data void areas over the globe.

5. REFERENCES

Conrath, B., R. Hanel, V. Kunde, C. Prabhakara, (1970). The Infrared Interferometer Experiment on Nimbus 3, J. Geophy. Res. 75, pp. 5831-5857.

Craig, R. A., (1965). The Upper Atmosphere. Meteorology and Physics, International Geophysics Series, Vol. 8, Academic Press, Inc., New York.

Deutsch, H. V. (1969). Atmospheric Ozone and Ultraviolet Radiation. Climamate of the Free Atmosphere — World Survey of Climatology, Vol. 4. New York: Elsevier, 1969, pp. 383-432.

Hovis, W. A., L. R. Blaine, and W. R. Callahan (1968). Infrared Aircraft Spectra Over Desert Terrain 8.5μ to 16μ. Appl. Opt., Vol. 7, p. 1137.

Koteswaram, P. (1958). The Easterly Jet Stream in the Tropics. Tellus, Vol. 10, pp. 43-57.

Krishnamurti, T. N., 1970. Observational Study of Tropical Upper Tropospheric Motion Field During Northern Hemispheric Summer. Rept. 70-4, Dept. of Meteorology, Florida State University, Tallahassee, 74 pp.

London, J., 1963. The Distribution of Total Ozone in the Northern Hemisphere. Beitr. Phys. Atmos., Vol. 36, pp. 254-263.

Murakami, T. (1958). The Sudden Change of Upper Westerlies Near Tibetan Plateau at the Beginning of Summer Season. Jour. Meteor. Soc. Japan, Vol. 36, pp. 239-274.

Murgatroyd, R. J., and F. Singleton (1961). Possible Meridional Circulation in the Stratosphere and Mesosphere. Quart. J. Roy. Meteor. Soc., Vol. 87, pp. 125-135.

Nimbus Project (1969). Nimbus 3 User's Guide, Goddard Space Flight Center, NASA, Greenbelt, Maryland, 238 pages.

Plass, G. N., (1958). Models for Spectral Band Absorption. Jour. Opt. Soc. Am., Vol. 48, pp. 690-703.

Prabhakara, C., B. J. Conrath, J. Steranka, and L. J. Allison, (1971). Nimbus 3 Satellite Observations of Ozone Associated with the Easterly Jet Stream Over India During the 1969 Monsoon. Proc. Indian Ocean Symp., Cochin, India.

Prabhakara, C., B. J. Conrath, R. A. Hanel, and E. J. Williamson, (1970). Remote Sensing of Atmospheric Ozone Using the 9.6 μm Band. Jour. of Am. Soc., Vol. 27, pp. 689-697.

APPENDIX

The spectral measurements made by the Infrared Interferometer Spectrometer, IRIS, onboard the Nimbus 3 satellite can be used to determine the total ozone content as was demonstrated by Prabhakara et al. (1970). There were two distinctly different steps involved in that procedure. First, the radiance measurements in the 15 μm CO_2 band were inverted to get the vertical temperature distribution (see Conrath et al. 1970), and then utilizing these temperature data we could get the information about the ozone from the IRIS radiances in 9.6 μm region by performing a second inversion. The radiance measurements in the window region around 10.5 μm were used to get the radiative brightness temperature of the earth's surface and the cloud tops that filled the field of view of IRIS. As this detailed two step inversion scheme is time consuming on the computer (IBM 360/91) we have developed a fast computational procedure which is essentially a statistical multiple regression scheme.

Ideally one should form multiple regression relations between Dobson total ozone measurements and the relevant IRIS radiances. But owing to the sparsity of Dobson measurements, that correspond to the exact time and geographic location of IRIS data, we were compelled to follow a different course. In the place of Dobson measurements we have substituted the total ozone values derived by our inversion procedure. As we had established earlier, with limited data, (see Prabhakara, et al., 1970) that the inversion method could estimate the total ozone accurate to 6% with respect to Dobson measurements, we feel this procedure is a reasonable one. In the ensuing discussion the words "total ozone" specifically mean the total ozone deduced from inversion.

A preliminary attempt was made to get linear multiple regression relations between total ozone and the various IRIS radiances listed in Table 1. In this way we could estimate the total ozone with a standard error of about 8%. This somewhat large error could be attributed to the inability of a simple linear procedure to simulate the physics of radiative transfer that is contained in the inversion scheme.

In order to improve the situation we have added some nonlinear terms to the regression scheme and tried to simulate the physics in an empirical fashion.

The radiative transfer equation which forms the basis for most of the remote sounding techniques may be written as

$$I = B_0 \tau_0 + \int_{\tau_0}^{1} B \, d\tau \qquad (1)$$

where I is the spectral intensity,

B_0 and B are the Planck intensities emitted at the ground and at any point in the atmosphere respectively,

τ_0 and τ are the transmissions from the ground and from any point along the vertical, to the top of the atmosphere respectively.

The transmission function τ applicable to the inhomogeneous path of ozone in the earth's atmosphere can be expressed with a complicated formalism (Prabhakara, et al. 1970). However, since ozone is present in the atmosphere only in trace quantities (a few parts per million) the absorption in the 9.6 μ ozone band follows a "weak line approximation" (Plass, 1959). As a consequence

Table 1

Regression Coefficients Used To Calculate the Total Ozone From the IRIS Radiances

No.	Wave No.* (cm^{-1})	Tropics (25°N to 25°S)			High Latitudes (25°N to 80°N and 25°S to 80°S)		
		α	β	γ	α	β	γ
1	668	+0.00217	+0.02499		+0.00144	+0.02040	
2	675	-0.00849	-0.70588		+0.00251	-0.08439	
3	680	-0.00126			-0.00093	-0.05624	
4	685	+0.00483	+0.38418		+0.00110	+0.05213	
5	690	-0.00056			-0.00479	-0.20379	
6	695	-0.00028			-0.00310	-0.12464	
7	700	+0.00498	+0.30060		+0.00463	+0.23824	
8	705	-0.00119			-0.00029	+0.05159	
9	710		-0.03210		-0.00263	-0.10858	
10	760				+0.00485		
11	955	+0.00098			+0.00316		
12	960				+0.00125		
13	965	-0.04643		+4.08446	-0.00218		+0.26841
14	970	+0.01466		-1.17229	-0.01654		+1.13984
15	975	+0.00454			+0.00017		
16	980	+0.00060			+0.00232		
17	985				-0.00057		
18	990	+0.00156			+0.00097		
19	995	-0.00176			-0.00214		
20	1000	+0.01899		-1.38051	-0.00088		-0.00436
21	1005	-0.00124			-0.00122		
22	1010	-0.00076			-0.00150		
23	1015	+0.01721		-1.05937	+0.00790		-0.39640
24	1020	-0.00089			+0.00139		
25	1025	-0.00179			-0.00180		
26	1030	+0.01292		-0.71877	+0.00883		-0.43834
27	1035			-0.08307	-0.00093		-0.07445
28	1040	-0.00139			-0.00048		
29	1045	-0.00146			-0.00068		
30	1050	-0.01244		+0.47771	+0.00067		-0.05286
31	1055	+0.01167		-0.55008	+0.01100		-0.33445
32	1060	-0.00162			-0.00188		
33	1090.8						
34	1122.1						
35	1155.5						
36	1201.4						
37	1230.6						

*The wave number indicated in the table corresponds to the center of a spectral interval of 5 cm^{-1} width. This width is determined by the spectral resolution of IRIS on Nimbus 3.

the weighting function, $d\tau/dz$, essentially resemble the ozone profile itself. Recognizing this basic simplicity we have attempted to approximate the transmission function with a simple expression as shown in Equation (2).

$$\tau_0 \cong \text{Exp} - \left[kO_3^T\right] \tag{2}$$

where k is some effective absorption coefficient and O_3^T is the total ozone content in the atmosphere.

Further following the chain of arguments given above, the radiative transfer Equation (1) can also be approximated as

$$I \cong B_0\tau_0 + \bar{B}\left(1 - \tau_0\right) \tag{3}$$

where

$$\bar{B} = \int_{\tau_0}^{1} \frac{B d\tau}{d\tau} .$$

Substituting the approximate expression for τ_0 given by Equation (2) into (3), rearranging terms, and taking logarithms we get

$$O_3^T = \frac{1}{k}\left[\log_e\left(B_0 - \bar{B}\right) - \log_e\left(I - \bar{B}\right)\right] \tag{4}$$

We have adapted the physical ingredients of Equation (4) into our multiple regression scheme. Finally, combining the linear and logarithmic terms involving the intensities at the various wave numbers listed in Table 1, we obtain the following regression equation.

$$O_3^T = C + \sum_{i=1}^{32}\left(I_i\alpha_i + \log\left(I_{10} - I_i\right).\beta_i + \log\left(I_i\right).\gamma_i\right) \tag{5}$$

where the subscript i indicates serial number of the spectral interval (of 5 cm^{-1} width) shown in Table 1,

α_i, β_i, and γ_i (see Table 1) are the coefficients of the expansion terms in the regression equation.

C is a constant of the regression equation.

The coefficients in Equation (5) are determined with the help of a multiple regression scheme.

In the inversion procedure of Prabhakara et al. (1970) the tropical latitudes (between 30°N and 30°S) and higher latitudes were treated as two distinct zones. In order to retain the same classification in the regression scheme we have developed two sets of coefficients one applicable to the tropics and the other to the higher latitudes.

The two sets of coefficients are given in Table 1. One can notice there are only 33 coefficients in the tropical set while the other set has 49. The number of variables chosen in the two cases were adequate to estimate the total ozone with a standard error less than 2%.

Reducing the error from 8% to 2% makes the ozone data useful for meteorological studies as the day to day changes in ozone are only about 10%.

Although we have two different zones, the tropics and the higher latitudes, it is desirable to have a smooth transition from one to the other. Such a transition is effected in the region between 25°-30° latitude in both the hemispheres by a simple weighting procedure.

We have so far not indicated some of the difficulties inherent in the estimation of ozone from the radiance measurements. There are principally two factors that can cause problems, (1) the emissivity of the surface or cloud tops, and (2) the extremely high clouds with cold temperatures at their top.

As no part of the 9.6μ ozone band is completely opaque to the radiation coming directly from the ground or cloud tops, we run into problems if the emissivity of these surfaces differ from one frequency to the other within the band. In fact, the emissivity of several types of soils and also clouds can be a function of frequency. Particularly over the desert regions the restrahlen bands (Hovis, 1968) due to sands interfere with the 9.6μ ozone band. To avoid these problems of emissivity we have developed an objective procedure to discard such data. The mean radiative brightness temperature of the spectral intervals 33 to 37 (see Table 1) on the short wave length side, and the mean brightness temperature of the spectral intervals 11 to 16 on the long wavelength side of the 9.6 μm ozone band are compared. If these two brightness temperatures differ from one another by 2% or more we have rejected the data.

When the field of view of IRIS is filled with high clouds having cold tops (<240°K) the 9.6μ region of the spectrum, which commonly appears as an absorption band, may appear as an emission band. In order to handle such circumstances we will need another set of regression coefficients. Since the physics involved behind such emission spectra is not completely known and since such high clouds occur only occasionally, we have rejected such data.

Finally to assess the accuracy of the ozone data derived from our regression procedure we have extracted a sample containing 200 of these regression ozone

data over the period of April 18 to July 22 to which the corresponding Dobson measurements were available. The spatial correspondence between the two sets of data is within 120 miles and the times agree within 24 hours. Measurements were taken from stations as far north as Resolute (74°N) to as far south as Wellington (41°S). A correlation coefficient of 0.85 was obtained between the two sets of data which yielded a standard error of estimate of 8%.* Since the tropical regions have usually smaller day to day variations we have partitioned the data and ran a separate correlation for the tropics only. This sample was small, about 50, and the correlation was disappointingly low 0.3. At the present time it is not possible for us to conclusively say which set of data, Dobson or regression, are unreliable. It is possible the Dobson measurements may have systematic differences from one station to the other in addition to some random errors in measurements. As we have no way of examining the nature of these Dobson measurements we have examined only our data for their consistency. In the IRIS determination of ozone, either by inversion or by multiple regression, the clouds constitute the single most important source of error. So we have subjected the tropical sample containing 50 IRIS measurements to a further test. In the test the IRIS ozone measurements are correlated with the corresponding window (950-980 cm^{-1}) brightness temperatures, which depend on the amount and the height of the clouds. A correlation coefficient of 0.22 was obtained suggesting that the clouds do not significantly affect the IRIS ozone measurements.

*It is desirable to correlate the satellite ozone measurements and Dobson measurements at each station. Such a procedure would restrict the correlation of the data in time avoiding all spatial variations. At present we have no more than 10 simultaneous measurements at any given station. For this reason we have not been able to make a meaningful correlation at any single station.

Also from the consistency of our ozone data, over the tropics, that we have observed in drawing the global maps of ozone, for April, May, June and July, 1969, makes us believe the IRIS data are reasonably sound.